Posttest Analyses of the 1:6 Scale Reinforced Concrete Containment

Phillip A. Pfeiffer, James M. Kennedy
Argonne National Laboratory, Argonne, IL USA
A. H. Marchertas
Northern Illinois University, Dekalb, IL USA

INTRODUCTION

A prediction of the response of the Sandia National Laboratories 1:6-scale reinforced concrete containment model test was made by Argonne National Laboratory. ANL along with nine other organizations performed a detailed nonlinear response analysis of the 1:6-scale model containment subjected to overpressurization in the fall of 1986. The two-dimensional code TEMP-STRESS (Marchertas, 1984) and the three-dimensional NEPTUNE (Kulak, 1985) code were utilized (1) to predict the global response of the structure, (2) to identify global failure sites and the corresponding failure pressures, and (3) to identify some local failure sites and pressure levels. A series of axisymmetric models was studied with the two-dimensional computer program TEMP-STRESS. The comparison of these pretest computations with test data from the containment model has provided a test for the capability of the respective finite element codes to predict global failure modes, and hence serves as a validation of these codes. Only the two-dimensional analyses will be discussed in this paper.

Three axisymmetric models have been analyzed (Pfeiffer et al., 1987) and two are displayed in Figures 1 and 2. The first (Figure 1) is a simplified model which only represents the cylindrical and spherical containment shell and omits the basemat. The latter is included in the two more complex models. The complex models also include representations of the foundation and sliding interfaces which permit separation and sliding between components of the basemat and the basemat and foundation. The three two-dimensional models all indicated failure at 180-185 psig. However, the three models predicted three different failure mechanisms: (1) hoop failure of the vessel at midheight following failure of a splice in this area, (2) failure of a weld in the liner near the basemat due to excessive strains, and (3) failure of the liner just above the knuckle due to compression failure of the concrete. More detail is available in Pfeiffer et al., 1987.

COMPARISON OF COMPUTED RESULTS WITH EXPERIMENTS

A low- and high-pressure test of the containment was completed in July 1987. The low pressure test was a structural integrity test (SIT), in which the containment was subjected to 53 psi. Crack mapping, displacements, and strains were recorded at various pressures. The purpose of the high pressure test was to determine the ultimate failure pressure. As in the SIT, displacements and strains in the containment were recorded at various pressures.

The experimental results of the high pressure test indicated a maximum internal pressure of 145 psig. Failure occurred due to the liner ripping at various locations, which resulted in the release of internal gases through the concrete and decrease in internal pressure. The locations of failure are around

equipment hatches and penetration insert plates, which are at the midheight of the vessel. This agrees with the results of the analyses, which indicated that the concrete is heavily cracked at these locations; once the liner rips, the pressure will decrease. The major reason that the analyses predicted a higher failure pressure than observed was that the axisymmetric models only capture the global response. Details of hatches and insert plates which cause the stress concentrations, would have to be analyzed through local models. However, the global models do predict the experimental displacement and strain response (away from the penetrations) of the vessel quite well.

A comparison of the response data and the pretest predictions is given in Figures 4-10. Most of the comparisons are for the first model, shown in Figure 1, which is titled "R. C. SHELL" in these figures. In some cases where this model was inappropriate for a reasonable comparison, the second model, shown in Figure 2, was used and titled "R. C. SHELL AND BASEMAT". As reference, the elevations and azimuthal angles are given in Figure 3.

The radial displacements of the liner are given in Figures 4 and 5 for elevations of 13 and 20.1 feet, respectively. Vertical displacements of the liner are given in Figures 6 and 7 for elevations of 11 feet and the springline, respectively. Figure 8 is the basemat uplift.

A very good comparison between the experimental and numerical results is obtained for the radial displacements. The nonlinear response due to plasticity in the rebar and liner is modelled quite well and is evident after 125 psi in the plots. Figures 4 and 5 show a distinct jump between 40 and 50 psi in the pretest predictions. This jump is attributed to pronounced hoop crack formation in the concrete throughout the structure's thickness with very little softening, that is, the cracks open up completely and develop fully. However, the experimental results do not indicate this type of behavior. A reasonable agreement for the vertical displacements is obtained only after the pressure reaches about 125 psi, although the numerical results are significantly shifted to the right of the experimental data. This discrepancy probably originates from the same cause as the jump in the numerical results in the radial displacements. In the vertical response, it was observed numerically that concrete cracking in the meridional (axial) direction occurred for pressures of approximately 40 to 115 psi. The experimental data does not support this observation. This lack of observed cracking will be further discussed. The basemat uplift, which was depicted in Figure 8 indicates that this absence of observed cracking could explain many of the differences in results. However, in spite of those caveats, the overall agreement is sufficiently good for most engineering purposes.

Maximum principal strains of the liner are given in Figure 9 for an elevation of 13.1 feet. When the maximum principal strain is compared, the direction of the strain cannot be easily depicted in the plot. In most cases the dominant strain is the hoop strain, however some axial strain effects near the springline are present (not shown). The dominance of the hoop strain can be observed from the figure because the strain jumps between 40 and 50 psi just like it did before for the radial displacements of the liner. After the strain jump, the experiment and the pretest predictions for the maximum principal strains compare favorably. The meridional rebar strains are given in Figure 10 for an elevation of 13.2 feet. In general, the vertical rebar strains agree only after the pressure reaches about 125 psi. Even after this pressure the numerical results are shifted to the right of the experimental data. This trend was also noticed in the vertical displacement response discussed earlier for the pretest results.

PRE-CRACKED BEHAVIOR

In general, good agreement was observed between the analytical prediction and the test results regarding the global behavior of the structure. A number of notable discrepancies between the analysis and test data were observed, the most

apparent of which was in the vertical displacement, meridional rebar strains and in the uplift of the basemat for the containment.

One possible explanation for the discrepancy is that the test structure was "precracked" before the test. This possibility was pursued by analyzing a shell model (Figure 1) which completely neglected the tensile strength of the concrete. This model assumed that the tensile strength of the reinforced concrete was solely due to the reinforcement. It was found that this analytical model yielded significantly better agreement with the test data on vertical displacements and strains. The results of the analysis, labeled "STEEL SHELL", are plotted in Figures 4 through 10.

The main observations of the "STEEL SHELL" results when compared to the pretest results and the experimental data are the following:

1. In the radial displacements (Figures 4 and 5) the displacement jump between 40 and 50 psi is absent for the STEEL SHELL analysis. This is because the concrete is modelled as pre-cracked. In the higher pressure analysis (125 psi and up) of the STEEL SHELL the results are shifted to the left of the pretest analysis. Thus, the STEEL SHELL analysis provides a better comparison with the experimental data.

2. In the vertical displacements (Figures 6 and 7) the STEEL SHELL results are shifted up for the whole pressure range and shifted to the left for the higher pressure (125 psi and up) when compared to the pretest results. Also, the STEEL SHELL analysis compares very well with the experimental data, whereas the pretest analysis did not.

3. In the liner strains (Figure 9) the strain jump between 40 and 50 psi is absent for the STEEL SHELL analysis. The higher pressure results are shifted to the left of the pretest result. Other than the strain jump, the STEEL SHELL analysis compares as well as the pretest analysis against the experimental data.

4. In the meridional rebar strains (Figure 10) the STEEL SHELL results, in general, are shifted up for the whole pressure range and shifted to the left for the higher pressures (125 psi and up) when compared to the pretest results. Also, the STEEL SHELL analysis generally compares very well with the experimental data, whereas the pretest analysis did not.

It was believed initially that prooftesting (structural integrity test) of the containment model to 53 psig pressure was responsible for cracking of concrete or the loss of tensile strength. It was noted, however, that the vertical displacement discrepancy in that test was of the same magnitude. Thus, the loss of tensile strength of the model could not be attributed to the prooftesting (SIT) phase.

Because of the excellent agreement of the STEEL SHELL model results with the experiment, an explanation was sought for the low tensile strength of the concrete before the tests. Several reasons were suggested, namely shrinkage cracking which take place during the curing process of the concrete; and cracking during the diurnal thermal cycling as well as seasonal temperature changes.

In order to investigate the cracking possibility of the concrete structure due to diurnal temperature fluctuations, a shell model (Figure 1) for a thermo-mechanical analysis was set up. A sinusoidal temperature variation was imposed on the outside wall of the model with an assumed amplitude of 20°F for a 24 hour cycle. The inside temperature of the containment (liner) was initially at 70°F and allowed to change with transient thermal analysis. The coefficient of thermal expansion for both the steel and concrete were assumed to be 1.0×10^{-5}

in/in/°F. The resulting damage (hoop and meridional cracking) due to the outside temperature varying from a high of 90°F to a low of 50°F on the outside results in some damaged areas. In general the concrete is cracked (hoop and meridional) 2/5 of the thickness from the outside surface in the cylinder and cracked 1/5 of the thickness from the outside surface in the dome. Although the structure is not completely damaged from this one day hypothetical thermal cycle, there is no doubt that actual daily temperature fluctuations and seasonal changes will cause the structure to be somewhat pre-cracked or damaged. This pre-cracking will also enhance shrinkage cracking, by providing pathways for the moisture in the concrete to escape. We believe that the temperature effect and shrinkage are mainly responsible for the concrete being in a pre-cracked state.

Other reasons for the containment exhibiting a pre-cracked state might be due to differential thermal expansion between the reinforcing steel and the concrete; and/or poor (no) bonding of rebar with the concrete.

SUMMARY

The reason that the vertical displacements and meridional strains of the pretest predictions and the experimental data did not compare well was due to the actual structure being softer or less stiff. Even the SIT test (in which the structure was not cracked beforehand) exhibited the same trend. This indicates that the concrete was pre-cracked or the concrete and reinforcement bond was very low or even nonexistent. As a check, the two-dimensional model was re-run with zero tension concrete, with only the steel liner and rebar having tension strength capacity. The liner displacements and strains; and rebar strains of this altered model check very well with the experimental results.

In general, a very good comparison between the experimental and pretest predictions was obtained for much of the global behavior of the structure. Strain and displacement responses where major discrepancies existed between the analysis and observed test data could be explained by pre-cracking.

ACKNOWLEDGEMENTS

This work was performed under the auspices of the U. S. Department of Energy, Office of Technology Support Programs, under contract W-31-109-Eng-38.

REFERENCES

Marchertas, A. H. (1984). Thermo-Mechanical Analysis of Concrete in LMFBR Programs. Nuclear Engineering and Design, Vol. 82, No. 1, pp. 47-62.

Kulak, R. F. (1985). Three-Dimensional Fluid-Structure Coupling in Transient Analysis. Computers and Structures, Vol. 21, No. 3, pp. 529-542.

Pfeiffer, P. A., Kulak, R. F., Kennedy, J. M., Marchertas, A. H. and Fiala, C. (1987). Pretest Analysis - Argonne National Laboratory, in Round-Robin Pretest Analyses of a 1:6-Scale Reinforced Concrete Containment Model Subject to Static Internal Pressurization. Edited by D. B. Clauss, NUREG/CR-4913, SAND87-0891, Sandia National Laboratories, pp. 82-129.

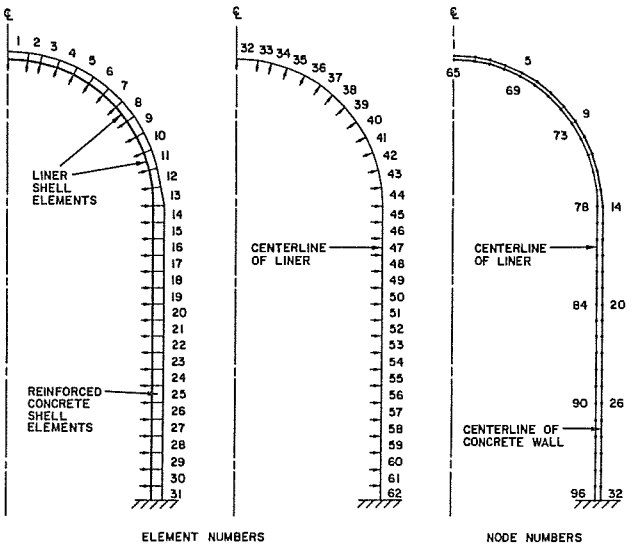

Figure 1. Discretization of Shell Model

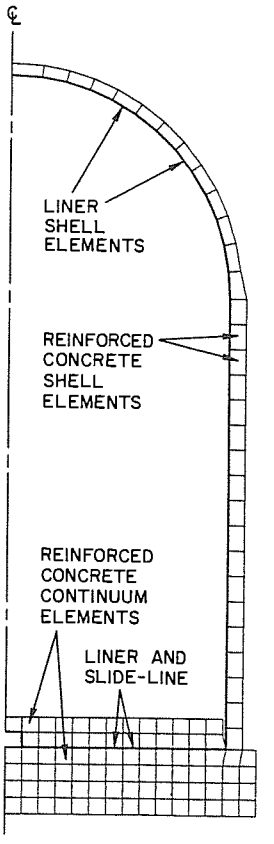

Figure 2. Discretization of Shell and Slab Model

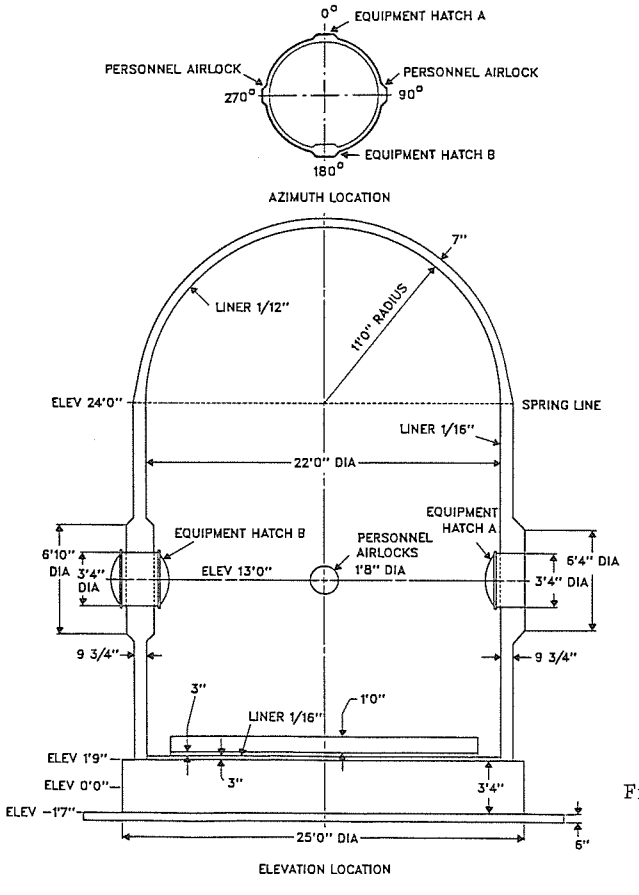

Figure 3. Schematic of the Containment Model

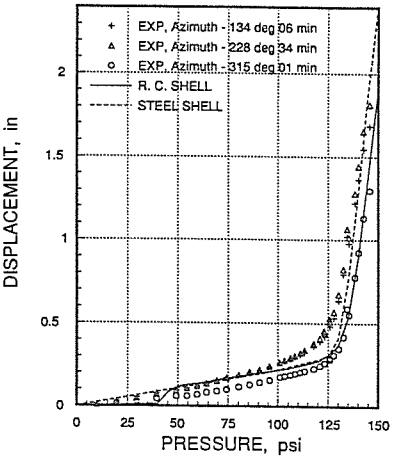

Figure 4. Radial Displacement of Liner at EL 13.0 ft

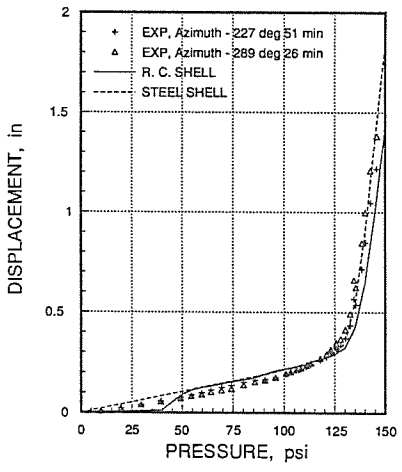

Figure 5. Radial Displacement of Liner at EL 20.1 ft

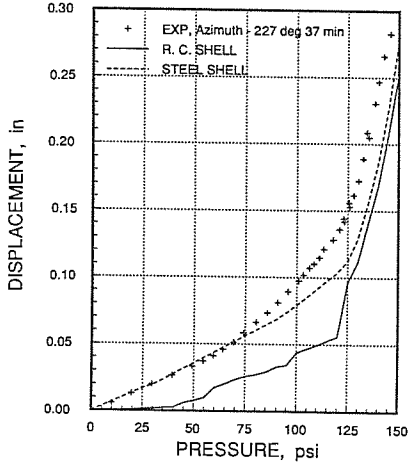

Figure 6. Vertical Displacement of Liner at EL 11.0 ft

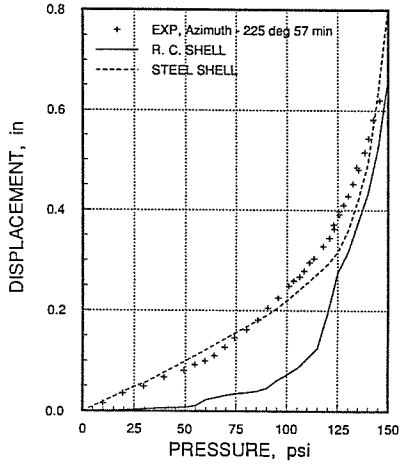

Figure 7. Vertical Displacement of Liner at the Springline

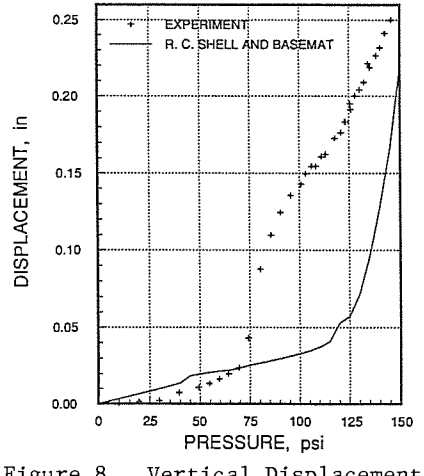

Figure 8. Vertical Displacement of the Basemat Uplift

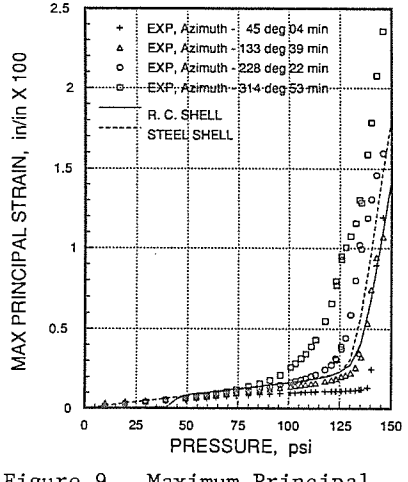

Figure 9. Maximum Principal Liner Strain at EL 13.1 ft

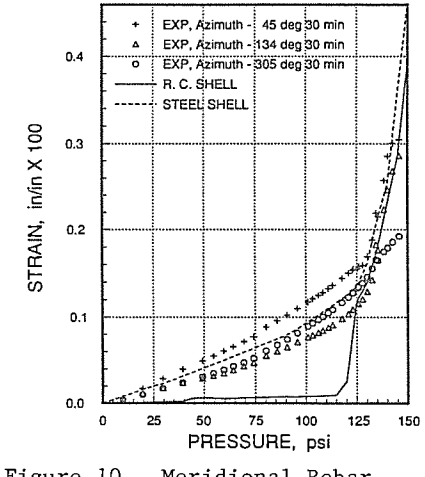

Figure 10. Meridional Rebar Strain at EL 13.2 ft